ADVANCED MATERIALS

DOI: 10.1002/adma.200600368

Growth of CdSe Quantum Rods and Multipods Seeded by Noble-Metal Nanoparticles**

By *Ken-Tye Yong*, *Yudhisthira Sahoo*, *Mark T. Swihart*,* and *Paras N. Prasad**

Semiconductor nanocrystals (NCs) have emerged as an important class of materials because of their tunable optoelectronic properties that arise from quantum size effects. They can be used as active components in functional nanocomposites,[1] chemical sensors,[2] biomedicine,[3–5] optoelectronics,[6,7] and nanoelectronics.[8–10] More recently, NCs of different shapes, including rods, bipods, tripods, tetrapods, and cubes[11] have been fabricated. These nonspherical NCs serve as ideal model systems for studying anisotropic optoelectronic effects, including polarized emission, and quantum rod (QR) lasing. They may also serve as building blocks for complex nanostructures in nanoelectronics and nanomedicine. Here, we report the preparation of CdSe QRs and multipods via heterogeneous nucleation on noble-metal nanoparticles. This allows their preparation at much milder conditions (225 °C, 0.066 M CdO) than previously reported (> 260 °C, > 0.4 M CdO). The CdSe NCs initially grow as multipods that subsequently cleave to form freestanding QRs with very high photoluminescence quantum yields (PL QYs).

Template-free shape control during the growth of NCs depends on the ability to achieve different growth rates on different crystal faces within the same NC. This occurs in an anisotropic crystal structure, such as the wurtzite structure of CdSe, when a single growth direction is favored over others. In this system, polymorphism is also possible, and a key parameter is the energy difference between different polymorphs.[12] In the case of CdSe and CdTe, NCs may nucleate with the zinc blende structure, followed by growth of the wurtzite structure[13,14] on these nuclei to produce tetrapods. The energy difference between the two crystal structures is small enough that both are accessible at typical reaction temperatures. This mechanism has been associated with the observation of kinetically promoted tetrapod structures of CdSe and CdTe.[12,15]

Generally, the colloidal growth of nonspherical NCs is achieved by one of two methods. In one approach, the reaction is carried out in the presence of two surfactants with significantly different binding abilities to the NC faces, such as phosphonic acid and a long-chain carboxylic acid or amine. The strongly adsorbed phosphonic acid slows the growth of the NC and results in a preferential growth along the *c*-axis of the wurtzite structure. In this method, a high precursor concentration is maintained, often via multiple injections of the precursors into the reaction pot during the growth of the NC. A mixture of carboxylic acid and amine, without a phosphonic acid, does not induce anisotropic NC growth, but yields spherical NCs[16] (Fig. S1 in the Supporting Information). Another approach is the solution–liquid–solid (SLS) method, analogous to the vapor–liquid–solid approach for growing nanowires from vapor precursors. This method uses metallic nanoparticles as seeds to promote anisotropic crystal growth.[17] The metallic seed particles melt, precursor atoms dissolve in them, and crystal growth occurs at the metal's liquefied surface. This provides a lower-energy path to nucleation than homogeneous nucleation in the vapor or solution phase. NC rods or wires of materials including InP,[18] InAs,[19] and Si[20] have been prepared using metallic nanoparticles as seeds. Growth of CdSe wires by the SLS method using bismuth-coated gold nanoparticles has been reported,[21] although those experiments were carried out using technical grade (90 %) trioctylphospine oxide containing phosphonic acids that may also promote anisotropic growth.[22] To the best of our knowledge, the use of pure noble-metal nanoparticles to aid the growth of nonspherical II–VI NCs has not previously been demonstrated.

Here, we report a single-pot colloidal synthesis of CdSe multipods and rods using nanoparticles of pure Au, Ag, Pd, or Pt as seeds. The CdSe multipods occur both as simple homogeneous multipods and as heteromultipods with the Au particle at the center of the structure (where Au is the seed), as shown schematically in Figure 1. The CdSe particles were produced using each type of metal nanoparticle (see Supporting

[*] Prof. M. T. Swihart, Prof. P. N. Prasad, K.-T. Yong, Prof. Y. Sahoo
Institute for Lasers, Photonics, and Biophotonics
University at Buffalo, The State University of New York
Buffalo, NY 14260-4200 (USA)
E-mail: swihart@eng.buffalo.edu; pnprasad@buffalo.edu
Prof. M. T. Swihart, K.-T. Yong
Department of Chemical and Biological Engineering
University at Buffalo, The State University of New York
Buffalo, NY 14260-4200 (USA)
Prof. P. N. Prasad, Prof. Y. Sahoo
Department of Chemistry, University at Buffalo
The State University of New York
Buffalo, NY 14260-4200 (USA)

[**] This work was supported in part by a Defense University Research Initiative on Nanotechnology grant, through the Chemistry and Life Sciences Directorate of the Air Force Office of Scientific Research and by an NSF grant from the Solid State and Polymer Chemistry Program of the Division of Materials Research. We also thank the staff at the National Center for Electron Microscopy for assistance with the HRTEM, and Paul Alivisatos and his group for helpful discussions. Supporting Information is available online from Wiley InterScience or from the author.

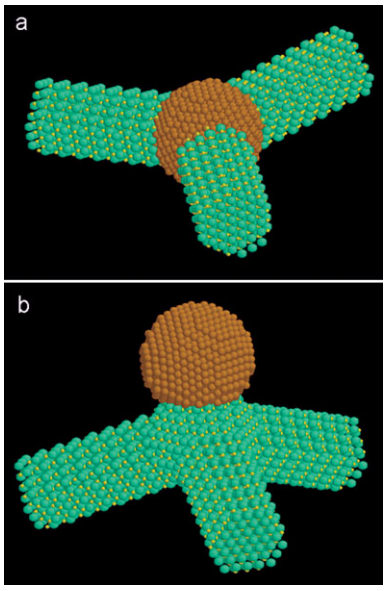

Figure 1. Schematic models of CdSe QR and tripod growth on a gold nanoparticle (Cd atoms are light green, Se atoms are yellow and Au atoms are gold). a) Heterotripod with CdSe basal planes aligned with the [111] planes of the gold nanoparticle. These can be brought into rough epitaxial registration over a distance comparable to the rod diameter. b) Nucleation of a zinc blende fragment on the surface of an Au nanoparticle (see also Table of Contents image), followed by growth of wurtzite arms to form a homotripod.

Information). In a typical reaction, cadmium oxide (1 mmol), myristic acid (3 mmol), and hexadecylamine (1 mmol) were added to 15 mL phenyl ether in a 250 mL three-necked flask. Freshly prepared metal nanoparticles (~0.05 mmol metal atoms) in an acetone–toluene mixture were added. The reaction mixture was slowly heated under an argon atmosphere to 220 °C, allowing the acetone and toluene to evaporate and CdO to dissolve, then maintained at 220 °C for 40 min. Then 0.5 mL of 1 M TOP-Se (ca. 0.5 mmol Se in 1.1 mmol trioctylphosphine) was rapidly injected. Samples were withdrawn after various reaction times and quenched with hexane. The samples were washed with acetone to remove excess surfactants, but no size selection was performed. The ratios of reagents, surfactants, and metal nanoparticles were the same in all experiments reported here. We refer to NCs seeded with Au, Ag, Pd, and Pt nanoparticles as CdSe(Au), CdSe(Ag), CdSe(Pd), and CdSe(Pt), respectively. The present approach does not use any phosphonic acids or trioctylphosphine oxide, the surfactants most often used for anisotropic growth of NCs. More importantly, the reaction temperature and reagent concentrations used here are much lower than those previously reported for CdSe rod synthesis (0.4 M, 260 °C).[23] The metal seed particles facilitate nucleation and growth of CdSe at these relatively mild conditions.

From transmission electron microscopy (TEM) image analysis, the estimated sizes of the Au, Ag, Pd, and Pt seed nanoparticles were 4.1±1.2, 7±1.1, 2.7±1.4, and 8.5±6.5 nm, respectively (Fig. S2). In the presence of any of these nanoparticles, the CdSe NCs were obtained as multipods (bipods, tripods, and/or tetrapods) and rods. Under exactly the same conditions, but without the metal nanoparticles, only spherical CdSe NCs were obtained (Fig. S1). The size and shape of the CdSe NCs depend on the choice of the metallic nanoparticles and the reaction time. CdSe(Au), CdSe(Ag), and CdSe(Pd), samples withdrawn during the first 3 min of reaction contained more multipod structures than rods (ca. 70 % multipods). However, the CdSe(Pt) samples always contained less than 5 % multipods (Fig. S3). Figure 2a–d shows TEM images of multipods produced after short reaction times using Au, Ag, Pd, and Pt nanoparticles as seeds, respectively (additional

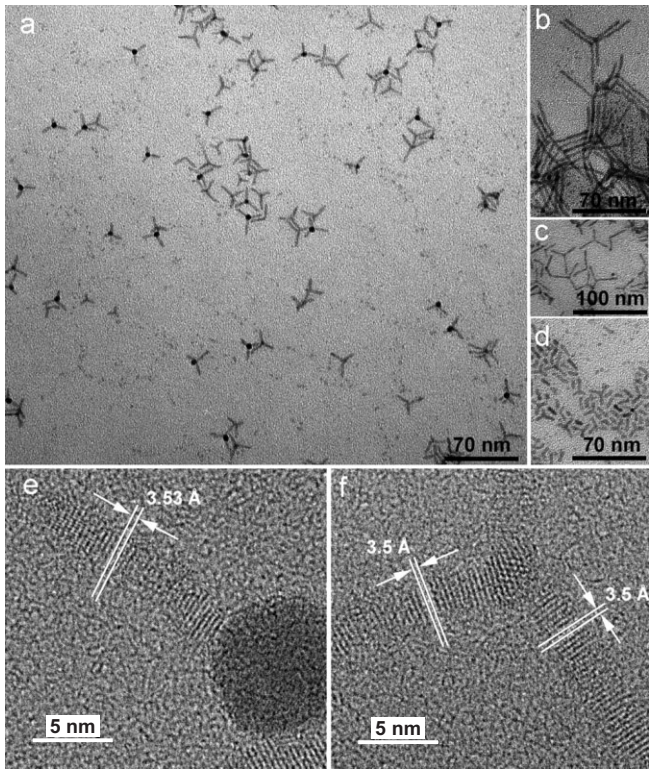

Figure 2. Bipods, tripods, and tetrapods, obtained after a short reaction time (ca. 3 min) in the presence of a) Au, b) Ag, c) Pd, and d) Pt nanoparticles. e) A high-resolution TEM (HRTEM) image of a single CdSe QR growing out of a gold nanoparticle (heteromultipod) and a pure CdSe tripod (homomultipod) with a lattice spacing of 3.5 Å.

images are shown in Fig. S4). Note that when Au seeds are used, an Au particle is sometimes present at the center of the multipod structure (a heteromultipod) although homomultipods constitute the dominant population (as shown for CdSe(Au) in Fig. 2a). However, homomultipods are the only multipods observed in other cases. For a given multipod, the arm lengths are nearly equal. For several repeated syntheses conducted for CdSe(Au), it was observed that most of the anisotropic growth took place during the first 2–3 min immediately after injection. The initial population of the multipods decreased and that of the rods increased significantly as the reaction progressed. After 20 min, the population was ca. 98 % rods. The rod diameters were quite uniform

ADVANCED MATERIALS

(ca. 10 % standard deviation in diameter, see Table S1 in the Supporting Information), whereas the rod length distribution was broader (standard deviation of 20 % or more, Table S1). The rod diameter and length distributions were not simply correlated to the seed-particle composition, size, or polydispersity. Most notably, in the case of the highly polydispersed Pt NCs, the multipods and rods retained fairly uniform rod diameters and lengths.

Figure 3 presents TEM images of the QRs of CdSe(Au), CdSe(Ag), CdSe(Pd), and CdSe(Pt) particles, from samples withdrawn after a longer reaction time (ca. 15–25 min). The QRs have lengths of 33.0±6, 30.0±6.7, 20.0±5.2, and 8.0±4.7 nm and diameters of 2.7±0.3, 3.0±0.3, 3.4±0.4, and 3.5±0.3 nm, respectively. The aspect ratio decreased slowly with increasing heating time, up to 40 min. Comparing Figures S4 and 3d we see that the aspect ratio of the CdSe(Pt) rods decreased from 3.7 after 3 min to 2.2 after 20 min. This suggests that further heating after depletion of the Cd—myristic acid precursor complex—results in ripening of the nanorods that would eventually reshape them into spheres. However, at the low reaction temperature used, this process is relatively slow. Such ripening was not observed at room temperature, where particle aspect ratios were stable for months. After reaction was complete, the noble-metal particles had detached from the rods (Fig. S6) and could be easily separated from the mixture through selective precipitation and centrifugation.

High-resolution TEM (HRTEM) (Fig. 2e and f) and powder X-ray diffraction (XRD) confirmed that the growth axis of the rods was the *c*-axis of the wurtzite structure. The powder XRD pattern of the CdSe QRs sample, with Au seeding, is shown in Figure 4. The diffractogram has the hexagonal wurtzite <100>, <002>, and <101> peaks of CdSe, with a dominant <002> peak[2] that is much less broadened than the other peaks, indicating longer-range order in that direction. No peaks due to Au are present, because a negligible amount of Au remains in the rodlike structures.

Absorption spectra (Fig. S7) of the multipods (Fig. S7a) and rods of all the NCs (Fig. S7b) show the expected structure with absorption onsets of 566, 589, 607, and 615 nm for CdSe(Au), CdSe(Ag), CdSe(Pd), and CdSe(Pt) nanorods, respectively. The absorption onset red-shifts with increasing rod diameter, and the emission Stokes shift increases with increasing aspect ratio, as expected for QRs. The PL QYs of CdSe(Au), CdSe(Ag), CdSe(Pd), and CdSe(Pt) QRs were 2.7, 10.9, 7.3, and 8.8 %, respectively. These QYs are much higher than the previously reported values for CdSe QRs. The QY could probably be further improved by depositing a shell of a larger-bandgap material (CdS or ZnS) on the QR, as shown previously.[24]

Metal particles have been used to induce one-dimensional NC growth in other systems, including CdSe and PbSe with Bi/Au core/shell material,[21,25,26] InAs with Au, Ag, or In,[17,19] and Si and Ge with Au.[20,27] In these cases, the growth is believed to occur via the SLS mechanism, first proposed by Trentler et al.,[28] in which the metal nanoparticles melt and serve as nucleation sites where a supersaturated precursor solution is converted into a crystalline product. The material being synthesized, or one of its components, dissolves in the droplet and is expelled at a single point in the form of a nanorod or nanowire. Simultaneous growth might occur at multiple points on the metal nanoparticle surface, giving rise to a heterogeneous multipod. In addition, the zinc blende crystal structure may nucleate on the surface of the metal particle itself, followed by growth of wurzite arms from the (111) faces of this nucleus, resulting in a homogeneous multipod (bipod, tripod, or tetrapod). In the present study, particles of Au, Ag, Pd, and Pt with bulk melting temperatures of 1064, 962, 1554, and 1768 °C, respectively, have been employed at temperatures below 225 °C. The formation of QRs is observed in all cases, indicating that something like the SLS mechanism is operative even at this temperature. However, it is highly unlikely that the seed particles are molten at the temperatures used here. Even accounting for size-dependent melting-point depression,[29] temperatures above 700 °C should be required to melt 4 nm gold seed particles. Significant quantities of cadmium can dissolve in the noble metals, and this alloying would also lower the melting point.[30] However, complete melting at 220 °C remains unlikely. Some molecular dynamic simulations of small metal clusters suggest that before the onset of melting, the relatively loosely bound surface atoms can undergo a surface-melting transformation,[31] which could make a SLS-type growth mechanism possible. Atomic surface and bulk diffusion coefficients are also size dependent, and are expected to be several orders of magnitude larger

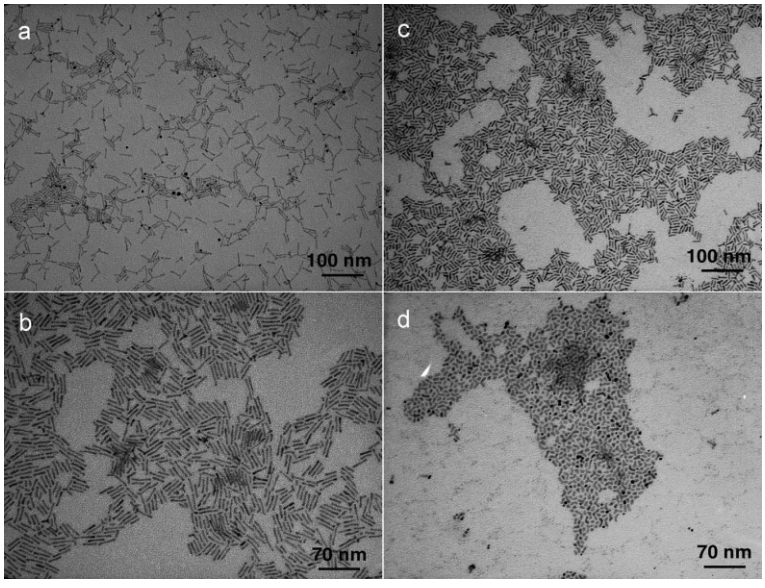

Figure 3. TEM images of QRs synthesized using a) Au, b) Ag, c) Pd, and d) Pt nanoparticles as seeds. Less than 2 % of the rods have branched structures.

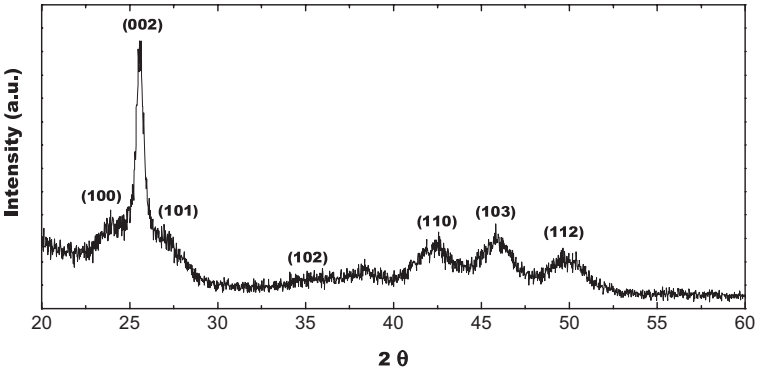

Figure 4. Powder XRD of CdSe (Au) rods. The 002 peak is narrower and more intense than other peaks due to the extended domain along the *c*-axis of the rod. The angles are measured in degrees.

in these nanoparticles than in the bulk.[29] This could enable a solid-state diffusion mechanism like that proposed by Persson et al.[32] for vapor–solid–solid growth of GaAs and InAs under conditions where the seed particles remain solid. Similarly, catalytically seeded growth of Si and Ge nanowires using solid seed particles has been reported to occur by a supercritical fluid–solid–solid mechanism.[27,33,34] In the present case, if the seed particle remains crystalline, then the rod growth may occur on particular crystal faces for which pseudoepitaxial growth is possible, as shown schematically in Figure 1. Because the lattice matching between the seed and the rod is only approximate, this pseudoepitaxy is possible only over a small rod diameter. This would explain the lack of correlation between the rod diameter and the seed particle diameter. In fact there is some limited correlation between the rod diameter and the lattice constant of the seed particle; Ag and Au, with lattice constants of 4.09 and 4.08 Å, respectively, produce somewhat smaller diameter rods than Pd and Pt, with lattice constants of 3.89 and 3.92 Å, respectively. This pseudoepitaxial growth could also lead to the observed cleavage of the NC from the seed particle, since the crystal strain energy in the growing NC, due to lattice mismatch, would increase with nanorod length. When this total strain energy exceeds a critical value, it will be thermodynamically favorable for the rod to cleave from the seed particle, relieving this strain at the expense of creating new interfaces.

We have recently reported the noble-metal seeded growth of PbSe rods,[35] and in that case we also observed that the semiconductor NCs cleave from the noble-metal seed particles. The mechanism in that case may have features in common with the present case, but there are also notable differences. For PbSe, the concentration of seed particles found to be effective in seeding growth of QRs is roughly a factor of 100 lower than that used here to seed growth of CdSe rods. While Cd has appreciable solubility in gold, Pb does not, so the solid-state diffusion mechanism that may be operative for CdSe is probably not possible in that case. Another obvious difference is that the wurtzite structure of CdSe is inherently anisotropic, and the preferred growth axis observed is aligned with the unique crystallographic direction. For PbSe, with the simple cubic (rocksalt) crystal structure, anisotropic growth is observed in spite of the fact that there is no such unique crystallographic direction. The commonalities and differences between these two systems remains an interesting topic for further investigation.

In summary, the present study shows that noble-metal nanoparticles can seed anistropic growth of high-quality CdSe NCs at lower temperature and reagent concentrations than have been used in other methods of preparing anisotropic CdSe structures. The resulting QRs have unusually high PL QYs. The ability to easily produce high-quality QRs in high yield and to control their shape in this way will be valuable in spectroscopic studies of the rods and in applications such as bioimaging technologies, light-emitting diodes, and photovoltaics.

Received: February 22, 2006
Final version: May 16, 2006
Published online: July 10, 2006

[1] C. A. Morris, M. L. Anderson, R. M. Stroud, C. I. Merzbacher, D. R. Rolison, *Science* **1999**, *284*, 622.
[2] J. Kong, N. R. Franklin, C. Zhou, M. G. Chapline, S. Peng, K. Cho, H. Dai, *Science* **2000**, *287*, 622.
[3] M. Bruchez, Jr., M. Moronne, P. Gin, S. Weiss, A. P. Alivisatos, *Science* **1998**, *281*, 2013.
[4] W. C. W. Chan, S. Nie, *Science* **1998**, *281*, 2016.
[5] T. A. Taton, C. A. Mirkin, R. L. Letsinger, *Science* **2000**, *289*, 1757.
[6] W. U. Huynh, J. J. Dittmer, A. P. Alivisatos, *Science* **2002**, *295*, 2425.
[7] V. I. Klimov, A. A. Mikhailovsky, S. Xu, A. Malko, J. A. Hollingsworth, C. A. Leatherdale, H. J. Eisler, M. G. Bawendi, *Science* **2000**, *290*, 314.
[8] X. Duan, Y. Huang, Y. Cui, J. Wang, C. M. Lieber, *Nature* **2001**, *409*, 66.
[9] M. S. Fuhrer, J. Nygard, L. F. Shih, M. Y. G. Yoon, M. S. C. Mazzoni, H. J. Choi, J. Ihm, S. G. Louie, A. Zettl, P. L. McEuen, *Science* **2000**, *288*, 494.
[10] M. S. Gudiksen, L. J. W. Lauhon, D. C. Smith, C. M. Lieber, *Nature* **2002**, *415*, 617.
[11] C. Burda, X. Chen, R. Narayanan, M. A. El-Sayed, *Chem. Rev.* **2005**, *105*, 1025.
[12] L. Manna, D. Milliron, A. Meisel, E. C. Scher, A. P. Alivisatos, *Nat. Mater.* **2003**, *2*, 382.
[13] Z. A. Peng, X. Peng, *J. Am. Chem. Soc.* **2001**, *123*, 183.
[14] W. W. Yu, L. Qu, W. Guo, X. Peng, *Chem. Mater.* **2003**, *15*, 2854.
[15] L. Manna, E. C. Scher, A. P. Alivisatos, *J. Am. Chem. Soc.* **2000**, *122*, 12 700.
[16] L.-S. Li, J. Hu, W. Yang, A. P. Alivisatos, *Nano Lett.* **2001**, *1*, 349.
[17] S. H. Kan, T. Mokari, E. Rothenberg, U. Banin, *Nat. Mater.* **2003**, *2*, 155.
[18] J. M. Nedeljkovic, O. I. Micic, S. P. Ahrenkiel, A. Miedaner, A. J. Nozik, *J. Am. Chem. Soc.* **2004**, *126*, 2632.
[19] S. H. Kan, A. Aharoni, T. Mokari, U. Banin, *Faraday Discuss.* **2004**, *125*, 23.
[20] J. D. Holmes, K. P. Johnston, R. C. Doty, B. A. Korgel, *Science* **2000**, *287*, 1471.

[21] J. W. Grebinski, K. L. Hull, J. Zhang, T. H. Kosel, M. Kuno, *Chem. Mater.* **2004**, *16*, 5260.
[22] X. Peng, L. Manna, W. Yang, J. Wickham, E. C. Scher, A. P. Alivisatos, *Nature* **2000**, *404*, 59.
[23] Z. A. Peng, X. Peng, *J. Am. Chem. Soc.* **2002**, *124*, 3343.
[24] L. Manna, E. C. Scher, L.-S. Li, A. P. Alivisatos, *J. Am. Chem. Soc.* **2002**, *124*, 7136.
[25] J. W. Grebinski, K. L. Richter, J. Zhang, T. H. Kosel, M. Kuno, *J. Phys. Chem. B* **2004**, *108*, 9745.
[26] K. L. Hull, J. W. Grebinski, T. H. Kosel, M. Kuno, *Chem. Mater.* **2005**, *17*, 4416.
[27] T. Hanrath, B. A. Korgel, *J. Am. Chem. Soc.* **2002**, *124*, 1424.
[28] T. J. Trentler, K. M. Hickman, S. C. Goel, A. M. Viano, P. C. Givvons, W. E. Buhro, *Science* **1995**, *270*, 1791.
[29] K. Dick, T. Dhanasekaran, Z. Zhang, D. Meisel, *J. Am. Chem. Soc.* **2002**, *124*, 2312.
[30] H. Baker, *ASM Handbook: Alloy Phase Diagrams*, ASM, Materials Park, OH **1992**.
[31] C. L. Cleveland, W. D. Luedtke, U. Landman, *Phys. Rev. B* **1999**, *60*, 5065.
[32] A. I. Persson, M. W. Larsson, S. Stenstrom, B. J. Ohlsson, L. Samuelson, L. R. Wallenberg, *Nat. Mater.* **2004**, *3*, 677.
[33] H. Y. Tuan, D. C. Lee, T. Hanrath, B. A. Korgel, *Chem. Mater.* **2005**, *17*, 5705.
[34] H. Y. Tuan, D. C. Lee, T. Hanrath, B. A. Korgel, *Nano Lett.* **2005**, *5*, 681.
[35] K.-T. Yong, Y. Sahoo, K. R. Choudhury, M. T. Swihart, J. R. Minter, P. N. Prasad, *Nano Lett.* **2006**, *6*, 709.

